$\rm EA01A/B: HIGH-RESOLUTION\; HI\; IMAGING\; OF\; AN\; INTERACTING\; PAIR\; OF\; POST-STARBURST\; (E+A)\; GALAXIES$

PIETER BUYLE¹, SVEN DE RIJCKE¹, HERWIG DEJONGHE¹

Draft version December 9, 2018

ABSTRACT

We present high spatial resolution 21 cm HI observations of EA01A and EA01B, a pair of interacting post-starburst, or E+A, galaxies at z = 0.0746. Based on optical HST/WFPC2 images, both galaxies are known to display disturbed morphologies. They also appear to be linked by a bridge of stars. Previous HI observations (Chang et al. 2001) had already uncovered sizable quantities of neutral gas in or near these galaxies but they lacked the spatial resolution to locate the gas with any precision within this galactic binary system. We have analysed deep, high resolution archival VLA observations of the couple. We find evidence for three gaseous tidal tails; one connected to EA01A and two emanating from EA01B. These findings confirm, independently from the optical imaging, that (i) EA01A and EA01B are actively interacting, and that, as a consequence, the starbursts that occurred in these galaxies were most likely triggered by this interaction, and that (ii) $6.6 \pm 0.9 \times 10^9$ M_{\odot} of neutral gas are still present in the immediate vicinity of the optical bodies of both galaxies. The H I column density is lowest at the optical positions of the galaxies, suggesting that most of the neutral gas that is visible in our maps is associated with the tidal arms and not with the galaxies themselves. This might provide an explanation for the apparent lack of ongoing star formation in these galaxies. Subject headings: galaxies: evolution, galaxies: elliptical, galaxies: ISM, galaxies: fundamental parameters

1. INTRODUCTION

Post-starburst galaxies (or PSGs, or E+A galaxies, or k+a/a+k galaxies) are characterized by their optical spectra, independent of any morphological or photometric considerations. PSGs contain a sizable population of very young stars, producing very prominent Balmer lines, but lack ongoing star formation, hence the absence of detectable emission lines. This suggests that PSGs are indeed observed very shortly, within less than 1 Gyr, after the end of a vigorous, abruptly truncated starburst (Dressler & Gunn 1983; Dressler et al. 1999; Poggianti et al. 1999). Today, they constitute only a small fraction of the galaxy cluster population (< 1\%, Fabricant et al. (1991); at intermediate-redshifts, however, they constituted a substantial cluster population (Belloni et al. 1995). Although the trigger and the abrupt end of the starburst is still not fully understood, photometry of PSGs shows evidence for disturbed morphologies, e.g. tidal tails, suggesting that in many cases the trigger is most likely associated to a galaxy-galaxy merger or interaction (Zabludoff et al. 1996; Yang et al. 2004; Blake et al. 2004; Tran et al. 2003; Goto 2005; Yang et al. 2008). Using numerical simulations, Bekki et al. (2005) has shown that PSGs can be formed via a major merger of two gas-rich spiral galaxies. In these merger simulations, a starburst is triggered that consumes the available gas within a timespan of roughly 1 Gyr, ending the starburst abruptly. Recent H I observations have uncovered large quantities of neutral hydrogen gas in a significant fraction of PSGs (Chang et al. 2001; Buyle et al. 2006; Helmboldt 2007; Buyle et al. 2008). This opens up the possibility of investigating the hypothesized merger origin of many PSGs.

Indeed, high-resolution interferometric radio observations of the neutral gas would provide valuable additional information. On the one hand, H I morphologies and velocity fields, if they are distorted, could corroborate the merger hypothesis, and, moreover, could reveal whether at least part of the neutral gas is still gravitationally bound and will remain available for future star formation. We selected the PSG binary EA01A/B as an interesting target for our study. Both galaxies have a PSGtype optical spectrum and have the same recession velocity. EA01A is the bluest galaxy of the PSG sample of Zabludoff et al. (1996), suggesting it is also the youngest sample member. HST/WFPC2 images in the F435W and F702W bands (Yang et al. 2004) provide strong evidence that the couple is interacting. EA01A, positioned about 11" east of EA01B, contains many stellar clusters that are very conspicuous compared with the overall rather low surface brightness of this galaxy. This diffuse appearance suggests it is on the verge of disintegrating due to the injected orbital energy. EA01B, on the other hand, is a bulge dominated early-type spiral galaxy; it sports strongly asymmetric stellar arms. Both galaxies appear to be connected by a stellar bridge. Previous HI observations (Chang et al. 2001) had already uncovered sizable quantities of neutral gas in or near these galaxies but they lacked the spatial resolution to locate the gas with any precision within this galactic binary system.

In section 2, we describe our data reduction and analysis of deep archival VLA H I observations of the EA01A/B galaxy binary. The results are presented and discussed in section 3 and summarized in section 4.

2. OBSERVATIONS AND DATA REDUCTION

We retrieved deep, high-resolution H I 21 cm observations of EA01A/B from the science archive of the

¹ Sterrenkundig Observatorium, Universiteit Gent, Krijgslaan 281, S9, B-9000, Ghent, Belgium; Pieter.Buyle@UGent.be, Sven.DeRijcke@UGent.be

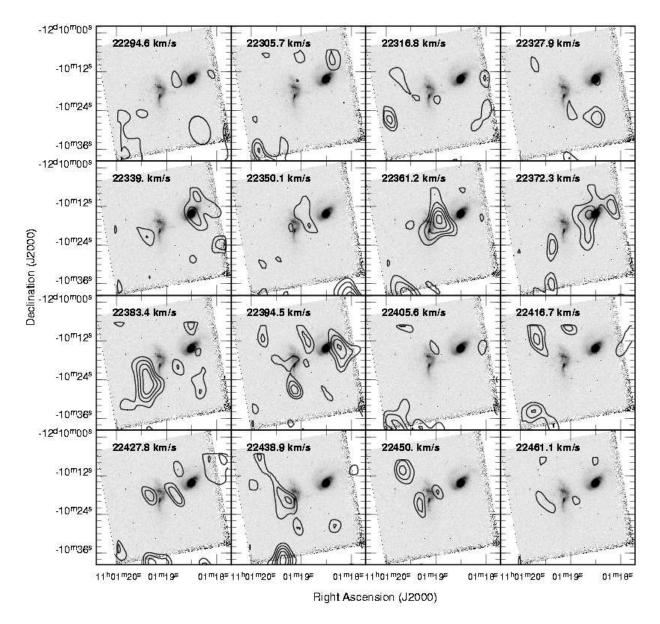


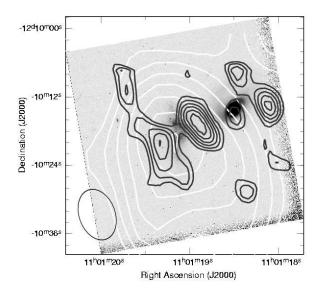
Fig. 1.— Channel maps overplotted on an optical HST/WFPC2 F702W image of EA01A/B. The contour levels are 2σ , 3σ ,... with σ =0.2 mJy beam⁻¹. The synthesized beam is depicted in the bottom-right corner of the first map (top left).

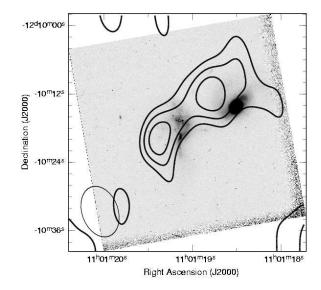
TABLE 1
Data characteristics

channel width (km s ⁻¹)	11.1
synthesized beam (FWHM)	$8.87'' \times 6.32''$
1σ noise level per channel	
flux density (mJy beam $^{-1}$)	0.2
brightness temperature (K beam ⁻¹)	2.1
column density ($\times 10^{19} \text{ cm}^{-2} \text{ beam}^{-1}$)	4.3
integrated 1σ noise level	
flux (Jy beam ^{-1} km s ^{-1})	0.01
brightness temperature (K beam $^{-1}$ km s $^{-1}$)	71.1
column density ($\times 10^{20} \text{ cm}^{-2} \text{ beam}^{-1}$)	1.9

National Radio Astronomy Observatory (NRAO), made with the Very Large Array (VLA) in New Mexico (USA) (project number AM0678). The observations were made with the B configuration during the nights of March 11, 12, 14, 16 and 18, 2001. At a central frequency

of 1321.76 MHz (L-band) and with a bandwidth of 3.125 MHz divided over 63 channels, the H I in EA01A/B was mapped with a velocity resolution of 11.1 km s^{-1} . Alternating observations of the phase calibrator 1127-145 with a 4 minute exposure time and EA01A/B with an exposure time of 25 minutes were made, followed at the end of each night by a 2.5 minute exposure of the flux calibrator 3C286. This resulted in a total on-source integration time of 32.6 h. Standard flagging and calibration of the u-v data was performed with the Astronomical Image Processing Software (AIPS). The continuum was subtracted by making a linear fit to the visibilities over the line-free channels that were not affected by the edge effects of the band. We created the final datacube using natural weighting to optimize the sensitivity. This yields a beam-size of $8.87'' \times 6.32''$ or $12.3 \ h^{-1} \ \text{kpc} \times 8.7 \ h^{-1} \ \text{kpc}$ at the angular-size distance of EA1 (D_A = $285 \ h^{-1}$ Mpc,





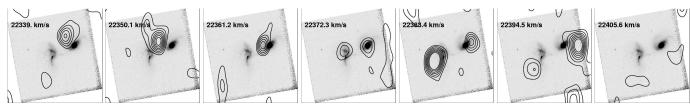


Fig. 2.— The observed H I flux integrated map (left panel) from Chang et al. (2001) (white contours) and from this paper (black contours) and the H I flux integrated map of a model that roughly reproduces the most conspicuous features of the channel maps (right panel). The synthesized beam is shown at the bottom left. The contour levels of the observed flux map correspond to 2σ , 3σ ,... with $\sigma = 0.01$ Jy beam⁻¹ km s⁻¹. The model channel maps are displayed in the bottom panels.

with $H_0 = 75 h \text{ km s}^{-1} \text{ Mpc}^{-1}$). The rms noise per channel is $0.2 \text{ mJy beam}^{-1}$, corresponding to a H I column density of $4.3 \times 10^{19} \text{ cm}^{-2}$ averaged over the beamwidth. A summary of the data characteristics can be found in Table 1.

3. DISCUSSION

We examined the final datacube and detected 21 cm emission in 12 adjacent channels, shown in Fig. 1. The H I flux integrated map of EA01A/B is presented in the left panel of Fig. 2. All maps are overplotted onto a HST/WFPC2 F702W image of the EA01A/B pair. It is clear from these maps that the H I emission spatially coincides with the optical position of EA01A/B and is centered around the heliocentric velocity of the previous H I detection and the optical recession velocity of the pair $(22327.9-22450.0\,\mathrm{km\,s^{-1}}).$

The H I profile of EA01A/B, obtained by summing the flux within a box covering the radio emission of the galaxy is plotted in Fig. 3. We fitted a Gaussian to the H I spectrum in order to derive the total 21 cm line flux. We generated a large library of mock H I spectra using this Gaussian model and added noise to produce synthetic data of the same quality as the original spectrum. We then fitted Gaussian profiles to the mock data in order to estimate the 1σ uncertainties on all relevant parameters. We find a total integrated flux of $S_{\nu}=0.26\pm0.03$ Jy km s⁻¹. This is equivalent to an H I mass of $M_{\rm HI}=6.6\pm0.9\times10^9$ M $_{\odot}$, adopting a luminosity distance $D_L=330$ Mpc. The central velocity of the Gaussian is 22357 ± 9 km s⁻¹ and its FWHM is

 $133 \pm 20 \; \mathrm{km} \, \mathrm{s}^{-1}$. We also re-reduced and analysed the low-resolution H I observations of Chang et al. (2001) (Fig. 2). Based on these data, we find a total integrated flux of $S_{\nu} = 0.29 \pm 0.08 \; \mathrm{Jy} \; \mathrm{km} \, \mathrm{s}^{-1}$, corresponding to an H I mass of $7.5 \pm 2.1 \times 10^9 \; \mathrm{M}_{\odot}$. The central velocity is $22371 \pm 30 \; \mathrm{km} \, \mathrm{s}^{-1}$ and the FWHM is $191 \pm 88 \; \mathrm{km} \, \mathrm{s}^{-1}$. This is in agreement with the high-resolution VLA data presented here and with Chang et al. (2001).

A plausible interpretation of the H I flux integrated map and the channel maps is that we are seeing one receding gaseous tidal arm emanating from EA01A and two tidal arms connected to EA01B, with the east arm approaching us and the west arm moving away from us. Little of the detected gas appears to be directly connected with the galaxies themselves, which show up as minima in the H I column density. This absence of dense gas may be related to the fact that these galaxies are in a poststarburst phase. The EA01A arm runs in a south-eastern direction and can be traced through 3 consecutive channel maps from $22372.3 \text{ km s}^{-1}$ to $22394.5 \text{ km s}^{-1}$. The west EA01B "arm" shows up as emission in 3 consecutive channel maps from $22372.3 \text{ km s}^{-1}$ to $22394.5 \text{ km s}^{-1}$. Following its position through adjacent channel maps with recession velocities below $\approx 22370 \text{ km s}^{-1}$, the east arm connected with EA01B appears to first shift in the direction of EA01A and then to return a position slightly north of EA01B before disappearing in the noise. At that point, the gas is moving towards us with a radial velocity of about 40 km s⁻¹, relative to the systemic velocity of EA01A/B. The curvature of the northern arm and the fact that it is approaching us agrees with the curvature

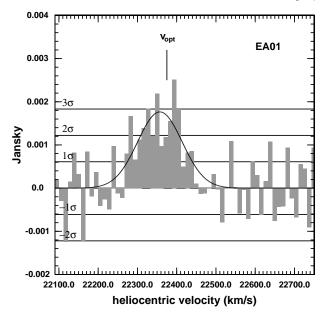


Fig. 3.— The H I profile of EA01A/B, obtained by summing the flux within a box around the flux integrated radio emission of the galaxy. Rms noise levels are indicated by horizontal lines. A Gaussian was fitted to the spectra to measure the velocity widths.

of the stellar arms.

Since the data quality clearly does not allow for a detailed or quantitative modeling of the gas distribution and kinematics, we constructed a very simplified model for the H I observations based on the interpretation outlined above. Two gaseous arms were constructed to emanate from EA01B, following the position and curvature of the stellar arms. If the ellipticity $\epsilon = b/a \approx 0.5$ of the outer isophotes of EA01B is indicative of its inclination, then this early-type disk is inclined by about 30° from an edge-on view. We assumed both arms to lie in a disk with the same inclination. A third gas arm was connected with EA01A, curving in a south-eastern direction. The H I flux density of these model tidal arms was assumed to decline exponentially with radius and they were given solid-body rotation velocity fields in such a way that the mock channel maps and the flux integrated map derived from this model provided an acceptable match to the observed maps, taking into account beam convolution and

added noise. Despite its simplicity, this model can give a fair account of the observations. The model flux map and channel maps are presented in Fig. 2 and can be compared with Fig. 1.

With a 2σ density limit of 4×10^{20} cm⁻² beam⁻¹, averaged over a $12.3~h^{-1}$ kpc×8.7 h^{-1} kpc beam, we cannot expect to trace the tidal arms very far out. As a comparison, under these conditions it would be impossible to trace the southern arm emanating from the interacting pair NGC4038/4039 ("The Antennae") further out than ~ 20 kpc (Hibbard et al. 2001). At the distance of EA01A/B, this corresponds to ~ 15", less than two beam diameters. At that distance, the velocity of the NGC4038/4039 tidal arm is less than ~ 50 km s⁻¹, in rough agreement with the largest velocities measured in the EA01A/B system.

4. CONCLUSIONS AND SUMMARY

EA01A/B is a close pair of post-starburst (E+A) galaxies, surrounded by some $7 \times 10^9 \ \mathrm{M}_{\odot}$ of neutral gas. Most of this gas resides in what appear to be three tidal arms, two of which are connected with EA01B. Together with optical HST/WFPC2 images, these observations show that EA01A and EA01B are actively interacting. The galaxies themselves show up as minima in the H I column density. This lack of galaxy-bound dense neutral gas is most likely connected with the fact that these galaxies are in a post-starburst phase.

We like to thank the referee, Tomotsugu Goto, for his very useful comments. PB and SDR are post-doctoral fellows of the Fund for Scientific Research - Flanders, Belgium (F.W.O.). The Very Large Array is a facility instrument of the National Radio Astronomy Observatory, which is operated by Associated Universities, Inc. under contract from the National Science Foundation. This work has made use of the NASA/IPAC Extragalactic Database (NED) which is operated by the Jet Propulsion Laboratory, California Institute of Technology, under contract with the National Aeronautics and Space Administration.

REFERENCES

Bekki, K., Couch, W. J., Shioya, Y., & Vazdekis, A. 2005, MNRAS, 359, 949 Belloni, P., Bruzual, A.G., Thimm, G.J. & Roser, H.-J., 1995, A&A, 297, 61 Blake, C., Pracy, M. B., Couch, W. J., Kenji, B., Lewis, I., Glazebrook, K., Baldry, I. K., Baugh, b. M., Bland-Hawthorn, J., et al., 2004, MNRAS, 355, 713 Buyle, P., Michielsen, D., De Rijcke, S., Pisano, D.J., Dejonghe, H. & Freeman, K. 2006, ApJ, 649, 163 Buyle, P., De Rijcke, S., Pisano, D.J., Michielsen, D., Dejonghe, H. & Freeman, K. 2008, ApJ, in preparation Chang, T., van Gorkom, J.H., Zabludoff, A., Zaritsky, D. & Mihos, C., 2001, AJ, 121, 1965 Couch, W. J., Sharples, R. M., 1987, MNRAS, 229, 423 Dressler, A., Gunn, J. E., 1983, ApJ, 270, 7 Dressler, A., Smail, I., Poggianti, B. M., Butcher, H., Couch, W. J., Ellis, R. S., & Oemler, A., Jr., 1999, ApJS, 122, 51

Fabricant, D.G., McClintock, J.E.& Bautz, M.W., 1991, ApJ,

381, 33

Franco, J., 2003, RMxAC, 15, 149 Goto, T. 2005, MNRAS, 357, 937 Helmboldt., J.F. 2007, MNRAS, 379, 1227 Hibbard, J. E., van der Hulst, J. M, Barnes, J. E., Rich, R. M., 2001, AJ, 122, 2969 Miller, N. A., & Owen, F. N. 2001, ApJ, 554, 125 Poggianti, B. M., Smail, I., Dressler, A., Couch, W. J., Barger, J., Butcher, H., Ellis, E. S., & Oemler, A., Jr., 1999, ApJ, 518, 576 Tran, K.-V. H., Franx, M., Illingworth, G., Kelson, D. D., & van Dokkum, P. 2003, ApJ, 599, 865 Yang, Y., Zabludoff, A. I., Zaritsky, D., Lauer, T. R., & Mihos, J. C. 2004, ApJ, 607, 258 Yang, Y., Zabludoff, A. I., Zaritsky, D. 2008, ApJ, submitted, arXiv:0801.1190 Zabludoff, A. I., Zaritsky, D., Lin, H., Tucker, D., Hashimoto, Y., Shectman, S. A., Oemler, A., & Kirshner, R. P. 1996, ApJ, 466,